Changes in Lysosome Shape and Distribution Correlated with Changes in Cytoplasmic pH

John Heuser

Washington University School of Medicine, St. Louis, Missouri 63110

Abstract. Lysosomes labeled by uptake of extracellular horseradish peroxidase display remarkable changes in shape and cellular distribution when cytoplasmic pH is experimentally altered. Normally, lysosomes in macrophages and fibroblasts cluster around the cell center. However, when the cytoplasmic pH is lowered to ~pH 6.5 by applying acetate or by various other means, lysosomes promptly move outward and accumulate in tight clusters at the very edge of the cell, particularly in regions that are actively ruffling before acidification but become quiescent. This movement follows the distribution of microtubules in these cells, and does not occur if microtubules are depolymerized with nocodazole before acidification. Subsequent removal of acetate or the other stimuli to acidification results in prompt resumption of ruffling activity and return of lysosomes into a tight cluster at the cell center. This is correlated with a rebound alkalinization of the cytoplasm. Correspondingly, direct application of weak bases also causes hyperruffling and unusually complete withdrawal of lysosomes to the cell center. Thus, lysosomes appear to be acted upon by microtubule-based motors of both the anterograde (kinesin) type as well as the retrograde (dynein) type, or else they possess bidirectional motors that are reversed by changes in cytoplasmic pH. During the outward movements induced by acidification, lysosomes also appear to be smaller and more predominantly vesicular than normal, while during inward movements they appear to be more confluent and elongated than normal, often becoming even more tubular than in phorbol-treated macrophages (Phaire-Washington, L., S. C. Silverstein, and E. Wang. 1980. *J. Cell Biol.* 86:641–655). These size and shape changes suggest that cytoplasmic pH also affects the fusion/fission properties of lysosomes. Combined with pH effects on their movement, the net result during recovery from acidification is a stretching of lysosomes into tubular forms along microtubules.

RECENT demonstrations of extended tubular lysosomes in macrophages and other cells (2, 16, 49, 56, 67, 72) has raised interesting questions about the mechanisms that control the shape and distribution of these intracellular organelles. Lysosomes have generally been viewed as discrete vesicular structures that tend to concentrate in and around the cell center (11, 12, 33, 68–71). For them to become tubules that radiate out from the cell center, they presumably have to fuse with each other and move outward by an active process. Experimental disruption of microtubules eliminates their outward radiation (72), suggesting that the active process may be a microtubule-based motor of the kinesin type, like the one that transports membrane organelles in an "anterograde" direction in neurons (7, 29, 36, 66, 78, 79). Lysosomes have long been known to accumulate centrally (4, 12, 13, 24, 25, 47), suggesting they have "retrograde" motors; however outward movements have only recently been detected (15, 23, 24, 41). The ultimate distribution and form of these pleomorphic organelles may thus boil down to a balance between membrane fusion and fission and between the activities of anterograde and retrograde motors.

Here, we describe several experimental protocols that appear to tip this balance toward lysosomal fission and outward movement. The protocols all produce a significant cytoplasmic acidification, to the range of ~pH 6.5. We also demonstrate that a converse alkalinization of the cytoplasm to the range of pH ~7.8 appears to "reset" the balance in the opposite direction, toward lysosome fusion into tubes and inward movement of the tubes. Although these experimental pH changes probably bypass or short-circuit normal cellular controls, we discuss how they may reflect and help to illuminate the normal mechanisms by which cells control their endosome and lysosome distribution.

Materials and Methods

Cell Cultures

Chick fibroblasts, mouse macrophages, and J774 cells were chosen for these experiments. The chick cells were second-generation primary cells, obtained by trypsin/EDTA resuspension of 1-wk-old cultures of homogenized chicken embryo pectoral muscle. The mouse macrophages were also second-generation primary cells, obtained by resuspension of 1-wk-old cultures of primary bone marrow cells grown in L-cell conditioned medium (e.g., medium containing CSF-1 to induce cell division and differentiation [10, 50]). The J774 cells are a permanent line of macrophage-like cells derived

Table I. Experimental Solutions

Ringer's solution: 155 mM NaCl; 5 mM KCl; 2 mM $CaCl_2$; 1 mM $MgCl_2$; 2 mM NaH_2PO_4; 10 mM Hepes buffer pH 7.2; 10 mM glucose; 0.5 mg/ml BSA

Tracers:
(1) Horseradish peroxidase (type VI; Sigma Chemical Co., St. Louis, MO) 5 mg/ml
(2) Lucifer Yellow (Type CH) 1 mg/ml
(3) Rhodamine dextran 1 mg/ml
(4) Rhodamine-tagged 0.2 μm polystyrene spheres 10^6/ml

Acidification media (following references 57, 58, 63, 75, 76):
(1) Acetate Ringer's: 80 mM NaCl, 70 mM Na acetate; 5 mM kCl; 2 mM $CaCl_2$; 1 mM $MgCl_2$; 2 mM NaH_2PO_4; 10 mM Hepes buffer pH 6.9; 10 mM glucose
(2) Na-free medium: 130 mM N-methyl-glucamine plus sufficient powdered acidic Hepes to bring pH to 7.2; 5 mM KCl; 2 mM $CaCl_2$; 1 mM $MgCl_2$; 1 mM KH_2PO_4; 10 mM glucose
(3) Nigericin (10 μM) in isotonic K medium: 50 mM K gluconate; 50 mM KCl; 30 mM Hepes buffered to pH 7.2 with KOH; 4 mM $CaCl_2$; 2 mM $MgCl_2$; 1 mM KH_2PO_4; 10 mM glucose
(4) Amiloride (1 mM) in normal Ringer's solution (above)

Alkalinization media (following references 5, 6, 59):
(1) NH_4Cl (10–30 mM) in normal bicarbonate-free Ringer's (above)
(2) Monensin or nigericin ionophores (1–10 μg/ml) in normal Ringer's
(3) Chloroquine, primaquine, or quinine (50 μM) in normal Ringer's

Fixation and HRP histochemistry buffer: 70 mM NaCl; 30 mM Hepes buffered to pH 7.2 with NaOH; 2 mM $CaCl_2$

Acid phosphatase histochemistry (all performed 60 min at 25°C, with stirring, and all washed afterwards for 10 min in 1% sodium sulfide in fix buffer, above, to blacken reaction product):
(1) (Gomori #1) 1 mg/ml cytidine 5′ monophosphate and 0.1% lead nitrate in 20 mM Tris-maleate buffer pH 5.0, plus 10 mM $MnCl_2$
(2) (Gomori #2) 25 mg/ml Na β-glycerophosphate and 0.1% lead nitrate in 40 mM Tris-acetate buffer pH 5.0
(3) (TPPase) 0.2 mg/ml Na-trimetaphosphate and 0.15% lead acetate in 50 mM acetate buffer pH 3.9

originally from a mouse tumor (52). All were plated onto 22-mm glass coverslips at 2.5 × 10^5 cells/ml in α-MEM containing 20% heat-inactivated fetal calf serum and the usual antibiotics.

Experimental Treatments

After 24–48 h in culture, before the cells began to approach confluence, they were removed from the CO_2 incubator and washed three times over 15 min in Hepes-buffered Ringer's solution containing 0.5 mg/ml bovine serum albumin (this solution is henceforth termed "Ringer's"; cf. Table I) to remove intracellular bicarbonate and allow their internal pH to drop back down to normal. Cells were then incubated in Ringer's plus one of the tracers listed in Table I, always for 20–30 min at 37°C with constant gentle stirring. After a 3–6-min wash in tracer-free Ringer's at 37°C, cells were transferred to one of the experimental solutions listed in Table I. After various intervals described below, they were transferred to 1.5% glutaraldehyde in the buffer indicated in Table I (henceforth termed "fixed buffer"), and fixed for 30 min at room temperature before being washed five times with fix buffer.

Histochemical Treatments

For horseradish peroxidase (HRP)[1] histochemistry, coverslips with cells fixed as above were incubated 15 min in 0.5 mg/ml diaminobenzidine in fix buffer, then 30 min in the same diaminobenzidine solution plus 0.01% H_2O_2 to initiate out the histochemical reaction (25). For acid phosphatase histochemistry, cells were fixed in 1.5% (wt/vol) paraformaldehyde rather than glutaraldehyde and reacted with one of the three mixtures indicated in Table I, according to published techniques (3, 45, 46).

Light Microscopy

After histochemistry, coverslips were given a final brief postfixation for 1 min in 0.2% OsO_4 in fix buffer, then dehydrated rapidly via two rinses in each of 70 and 100% ethanol and embedded in English Araldite epoxy resin by standard EM techniques (25). The Araldite served as a mounting medium to attach the coverslips to a glass slide, and yielded better cellular morphology and greater permanence than the usual light microscopic mounting media. After polymerization of the Araldite at 80°C for 24 h, coverslips were viewed with a 100× phase-contrast objective and photographed on Kodak T-Max ASA 100 black and white 35-mm film.

Results

Lysosome Movements Provoked by Cytoplasmic Acidification and Alkalinization

Endosomes and lysosomes were visualized by internalization of several different extracellular tracers (Table I), all applied in sufficiently high concentration to insure that most uptake would occur via bulk internalization rather than via receptor-mediated membrane binding. The duration of uptake (30 min, including subsequent washes) was sufficient to deliver these tracers to "late" endosomes or secondary lysosomes, i.e., to endosomes that presumably had time to acidify and acquire lysosomal enzymes (21, 44, 64, 71, 81). After tracer uptake, several different protocols of cytoplasmic acidification or alkalinization were applied (Table I). All generally provoked the same patterns of lysosome redistribution (Table II). Moreover, many additional cell types were studied, and in spite of major differences in the amount of tracer they internalized, all showed the same redistributions of lysosomes upon changing cytoplasmic pH. In no case did these movements require external calcium: they occurred promptly and completely in calcium-free Ringer's and they were not provoked by direct application of 5 μM of the Ca^{++}-ionophores A23187 or ionomycin in the presence of 2 mM external Ca^{++} (not shown).

The phase-contrast light micrographs in Figs. 1 and 2 typify the changes in shape and distribution of HRP-loaded organelles observed. Figs. 1 *a* and 2 *a* illustrate the normal condition of these organelles in primary and cultured macrophages after 20 min of loading and 10 min of washing away excess HRP. In such "control" cells, most lysosomes are concentrated near the cell center (Table II), and those in the periphery appear vesicular. Figs. 1 *b* and 2 *b* illustrate the effects of replacing 70 mM of the NaCl in the Ringer's with 70 mM of sodium acetate (pH 6.9): most of the HRP-loaded lysosomes move to the very edge of the cell. Simultaneously, the cell flattens out and loses most of its peripheral ruffles (compare arrows in Fig. 1 *a* and 1 *b*). (By time-lapse video-enhanced light microscopy, the remaining rim of ectoplasm in acidified cells is observed to be completely static.) Figs. 1 *c* and 2 *c* illustrate that a 15-min exposure to normal Ringer's after 15 min of such acetate treatment results in a return of HRP-loaded organelles to the cell center, as well as a rounding up of the cell and reappearance of unusually broad ruffles (compare arrows in Fig. 2, *b* and *c*). (Time-lapse microscopy at this point illustrates that such ruffles are

1. *Abbreviation used in this paper*: HRP, horseradish peroxidase.

Table II. Distribution of HRP-loaded Lysosomes in Mouse Bone Marrow Macrophages after 15-min Exposure to Various Acidification or Alkalinization Media

Treatment	Proportion of cells showing various distributions			
	Clustered around cell center	Clustered centrally with radiating tubules	Dispersed throughout cell	Dispersed with peripheral vesicle clusters
Control	0.75	0.15	0.05	0.05
Acetate Ringer's pH 7.4	0.40	0.10	0.35	0.15
Acetate Ringer's pH 6.9	0.05	0.05	0.30	0.60
Na^+-free media	0.10	0.10	0.45	0.35
Amiloride (1 mM)	0.20	0.10	0.40	0.30
Nigericin in isotonic K^+ pH 6.2	0.15	0.00	0.60	0.25
Isotonic K^+ alone pH 7.4	0.15	0.30	0.35	0.20
NH_4Cl (20 mM)	0.90	0.10	0.00	0.00
Monensin (10 μg/ml)	0.95	0.05	0.00	0.00
Chloroquine (20 μM)	0.20	0.55	0.05	0.20

In all cases, monolayer cultures were exposed to HRP for 30 min and then soaked an additional 15 min in one or another of the above media. Thereafter, 100 cells from two separate experiments were categorized single blindedly and the resulting proportions were rounded off to the nearest 0.05.

unusually active.) Fig. 3 illustrates comparable changes in chick fibroblasts. These are less dramatic because fibroblasts take up ~10-fold less HRP than do macrophages (68, 69, 71); nevertheless, their HRP-loaded organelles are normally clustered centrally after the 30 min loading period (Fig. 3 *a*), move outward in response to 70 mM acetate (Fig. 3 *b*), and return to the cell center upon washout of acetate (Fig. 3 *c*). Again, time-lapse microscopy illustrates a cessation of fibroblast ruffling during acidification and hyperactivity during recovery.)

Measurements of intracellular pH made on parallel monolayer cultures loaded with the pH-sensitive fluophore 2',7'-bis(carboxyethyl)-5,6-carboxyfluorescein (55) and analyzed by UV spectrofluorimetry, to be described in detail elsewhere (Schlesinger, P. H., and J. E. Heuser, manuscript in preparation), showed that immediately upon application of 70 mM acetate, cytoplasmic pH in mouse macrophages and chick fibroblasts falls to ~6.5 and remains there for the duration of the exposure. Upon washout of acetate, cytoplasmic pH immediately rebounds to ~0.5 pH units above normal (~pH 7.8) and then slowly falls back to normal over the next 10–15 min. The hyperactivity and unusually tight central clustering of HRP organelles seen during acetate washout (Figs. 1 *c* and 2 *c*) thus appear to correlate temporally with a period of rebound alkalinization. Correspondingly, direct alkalinization of macrophages by the addition of 10–20 mM NH_4Cl to their Ringer's raises their cytoplasmic pH by ~0.5 units and leads to the same structural changes in HRP-loaded organelles and ruffles as seen during acetate washout (Tables II and III). Experiments using nigericin "clamping" of cytoplasmic pH over a wide range (Fig. 4) indicate that there is not a pH threshold for this lysosome redistribution, but it oc-

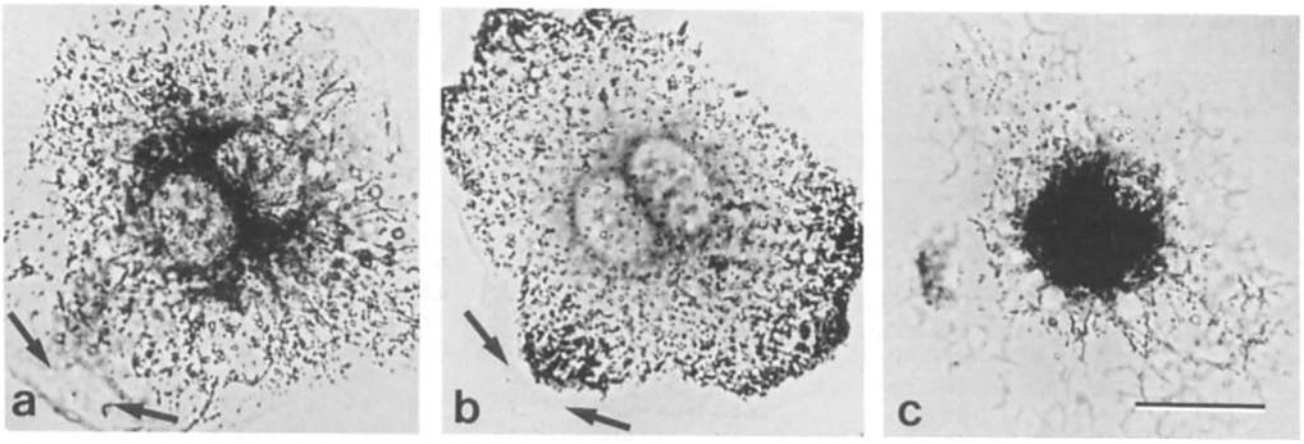

Figure 1. Reversal of normal lysosome movements in mouse bone marrow macrophages. (*a*) Control distribution of HRP-labeled lysosomes around the cell center after 30 min of tracer uptake; (*b*) peripheral migration of lysosomes after exposure to media containing 70 mM acetate for 15 min. (*c*) Return of lysosomes to the cell center in a macrophage exposed to acetate for 15 min (as in *b*) and then washed in normal Ringer's for 15 min. Arrows indicate associated loss of membrane ruffles during acidification, as discussed in the text. Bar, 20 μm.

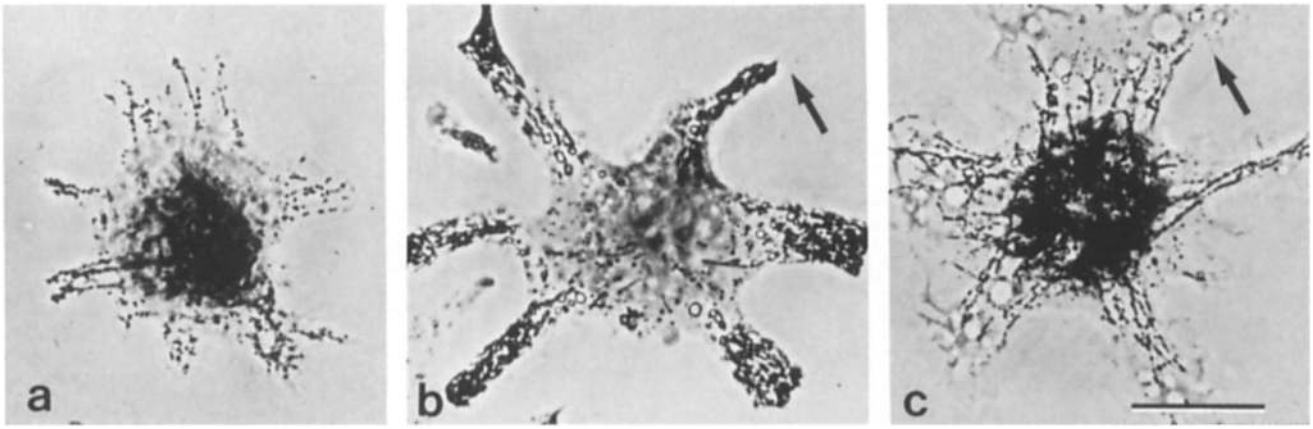

Figure 2. Rearrangements of HRP-labeled lysosomes in broadly spread J774 macrophages. (*a*) Control distribution after 30 min of HRP uptake; (*b*) peripheral distribution of lysosomal vesicles after exposure to 70 mM acetate for 15 min. (*c*) Central clustering of lysosomes with radiating tubules, 15 min after washout of acetate. Arrows illustrate associated increase in membrane ruffles during recovery, as discussed in the text. Bar, 20 μm.

curs progressively over the range of pH 6.6–7.3, with elimination of central clusters preceding establishment of peripheral clusters.

Identical organelle redistributions and shape-changes are observed in cells assayed for acid phosphatase rather than loaded with HRP (Fig. 5). Initially, acid phosphatase-stained organelles are clustered around the cell center (Fig. 5 *a*); after 15 min in 70 mM acetate, they are redirected to the distal margins of the cell (Fig. 5 *b*); and after 10 min of acetate washout they are back in the cell center (Fig. 5 *c*). Such acid phosphatase-positive organelles are presumably identical to the HRP-loaded organelles observed in Figs. 1–3 above, all qualifying for the name "secondary lysosomes."

Changes in Lysosomal Shape Correlated with Cytoplasmic pH

Table II documents that during acidification lysosomes also appear to be more vesicular than normal, while during rebound alkalinization (or during direct alkalinization with NH_4Cl; cf. Table III, line 6) they appear to be more tubular than normal. This is visible by comparing Fig. 2, *a* and *c* or Fig. 3, *a* and *c*, for example. The formation of tubules is particularly dramatic during the early phases of recovery, when tight central clusters of lysosomes have not yet fully reformed but are in the process of doing so. Fig. 6 *a* illustrates that long HRP-loaded tubules, extending all the way from the cell periphery to the cell center, can be found at this time. In some cases the tubules appear instead as closely aligned chains of vesicles (Fig. 6 *b*), an effect known to be produced by glutaraldehyde fixation (56, 72).

Role of Microtubules in Endosome Movements

Neither the abundance nor the distribution of microtubules in macrophages (Fig. 7) is altered by changes in cytoplasmic pH, nor by HRP uptake (not shown). To assess the role of microtubules in lysosomal redistribution patterns, HRP-loaded cells were treated with 2 μM nocodazole (5 min at 4°C, followed by 15 min at 37°C). Lysosomes appeared randomly distributed in such cells, and tubular forms were absent. Moreover, when such cells were acidified in the presence of nocodazole, lysosomes clumped locally but did not

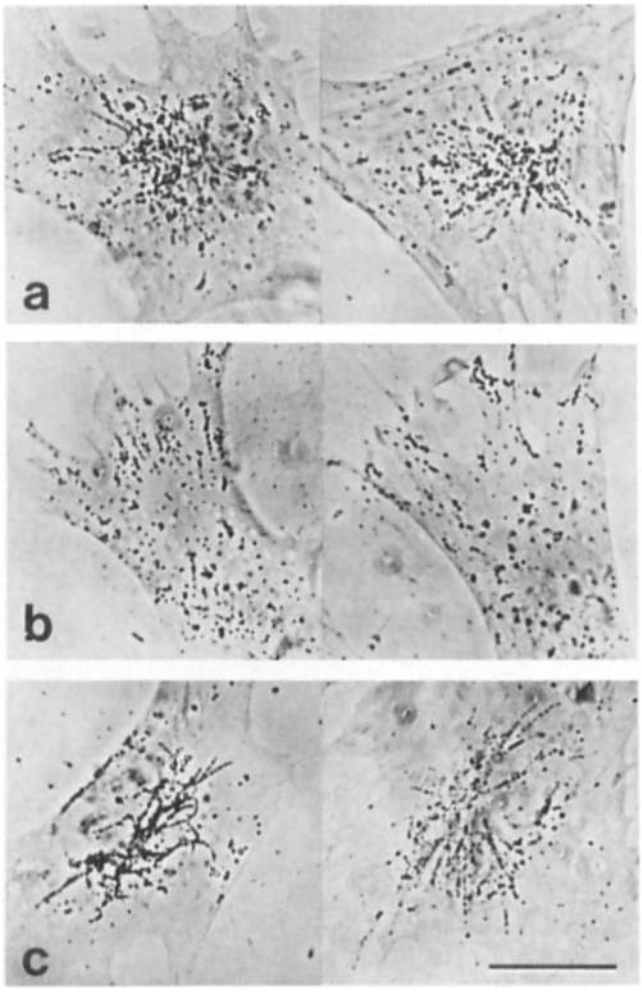

Figure 3. Centrifugal and centripetal movements of HRP-labeled lysosomes in cultured chick fibroblasts. (*a*) Lysosomes are clustered around the cell center in control cells after 30 min of labeling; (*b*) lysosomes have moved out of the cell center, occasionally in linear arrays, in cells exposed to 70 mM acetate for 15 min after HRP loading; (*c*) lysosomes have returned to the cell center, often in linear arrays, in acetate-treated cells that recovered in normal Ringer's for 10 min before fixation and HRP histochemistry. Bar, 20 μm.

Table III. Timecourse of Changes in Distribution of HRP-loaded Lysosomes in Mouse Bone Marrow Macrophages During Changes in Cytoplasmic pH

Treatment (and resultant cytoplasmic pH)	Proportion of cells showing various distributions			
	Clustered around cell center	Clustered centrally with radiating tubules	Dispersed throughout cell	Dispersed with peripheral vesicle clusters
(1) control (7.2–7.4)	0.75	0.15	0.05	0.05
(2) 5′ acetate (6.4–6.6)	0.20	0.00	0.55	0.25
(3) 15′ acetate (6.6–6.8)	0.05	0.05	0.30	0.60
(4) 5′ recover (7.8–8.0)	0.15	0.40	0.20	0.25
(5) 15′ recover (7.5–7.8)	0.40	0.35	0.15	0.10
(6) 5′ ammonia (7.8–8.0)	0.35	0.65	0.00	0.00
(7) 15′ ammonia (7.6–7.9)	0.90	0.10	0.00	0.00

In all cases, monolayer cultures were exposed to HRP for 30 min and then soaked an additional 15 min in normal Ringer's (line 1) or in Ringer's containing 70 mM Na acetate (lines 2 & 3). Lines 4 & 5 refer to cells that were loaded with HRP for 30 min and acidified with 70 mM Na acetate for 15 min before being returned to normal Ringer's for recovery periods of 5 or 15 min. Lines 6 & 7 refer to cells soaked in Ringer's containing 20 mM NH_4Cl after the usual 30 min of HRP exposure in normal Ringer's. For each treatment, 100 cells from 3 independent experiments were categorized single-blindedly and the resulting proportions were rounded off to the nearest 0.05.

display any net outward movement. Likewise, if cells were first acidified and then treated with nocodazole, the peripheral clusters of lysosomes dispersed. Subsequently, lysosomes failed to move back into the cell center when normal cytoplasmic pH was restored.

Organelles That Do Not Redistribute with Lysosomes During pH Changes

As noted above, acidified cells become flat and lose their ruffles, while recovering cells become unusually round and hyperactive. These effects may be related to changes in cytoplasmic viscosity: for example, phase-dense granules near the cell center display active Brownian movements in acidified cells but not in normal cells, as if released from passive constraints. Concomitant with these shape changes, organelles such as endoplasmic reticulum and mitochondria (detected by $DiOC_6$ staining; references 73, 74), phase-dense granules (presumably lipid droplets and residual bodies; references 11, 12), and Golgi elements (detected by anticlathrin monoclonal antibodies kindly provided by F. Brodsky, University of California, San Francisco) all appear to disperse somewhat during acidification (cell flattening) and gather together again during recovery (cell rounding). However, none of these organelles show the extreme changes in localization displayed by the lysosome system (Figs. 1–3). There is no indication that they undergo the same active movements.

Indications That "Early" Endosomes and Phagosomes Also Do Not Move

Certain types of endocytotic organelles also do not undergo the same microtubule-directed movements as lysosomes. The first are "early phagosomes," marked by rhodamine-tagged 0.2-μm latex beads. In one experiment, macrophages were exposed to Lucifer Yellow (1 mg/ml) for 30 min to preload the same compartments that were normally loaded with HRP, and were then exposed briefly to an acidifying medium that contained the rhodamine-tagged beads. After 5 min in this medium the cells were formaldehyde fixed and examined by fluorescence microscopy. This displayed the usual displacement of yellow lysosomes to the cell periphery (Fig. 8 *a*), but the recently formed red-bead phagosomes remained randomly distributed (Fig. 8 *b*).

A second experiment was then devised to determine whether this result was due simply to different rates of movement of large vs. small compartments (the red phagosomes being somewhat larger than the yellow lysosomes). Macrophages of fibroblasts were labeled with HRP for the usual 30 min but in the continuous presence of 70 mM acetate, which inhibits HRP uptake and leads to the appearance of relatively small HRP-containing inclusions (Fig. 9). Current thinking is that these are "early endosomes" that accumulate because cytoplasmic acidification prevents their maturation into later endosomes and lysosomes (14, 62, 81). Of interest here is the fact that these compartments remain randomly distributed in the cell, in spite of their relatively small size and the prolonged exposure to acidifying conditions. Acid phosphatase staining of parallel cells confirmed that lysosomes redistributed to the cell periphery as usual. If the HRP-containing organelles in this experiment are in fact early endosomes, their lack of response to pH changes may suggest that the ability to move may be a correlate of (if not a prerequisite for) endosome maturation.

Discussion

The microscopic observations presented here indicate that cytoplasmic acidification alters the normal distribution of secondary lysosomes around the cell center, apparently by provoking their outward movement along microtubules. This

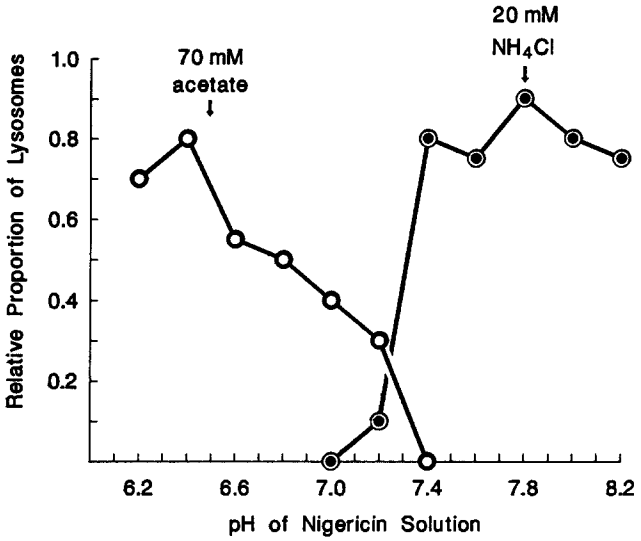

Figure 4. pH titration of lysosome distribution in nigericin-treated macrophages. Circles with dots in the center represent the proportion of cells with predominantly centralized lysosomes, while open circles represent the proportion of cells that displayed displacement of lysosomes into at least two distinct peripheral clusters. Monolayer cultures were first exposed to HRP in normal Ringer's for 20 min at 37°C and then incubated for 15 min in 1 μg/ml nigericin in isotonic K^+ media (Table I) buffered to the various values on the abscissa (using 2-[*N*-morpholino]ethane sulfonic acid [MES] buffer for pH 6.2–6.8, Hepes buffer for 7.0–7.6, and EPPS buffer for 7.8–8.2). After fixation and HRP histochemistry, 100 cells from two separate experiments were categorized single blindedly and the resulting proportions were rounded off to the nearest 0.05. (Not shown is the proportion of cells with neither peripheral nor central clusters, which brought the totals at each pH to 1.00. These were clearly the majority at pH 7.0–7.2). The lysosome pattern seen after 15 min in 70 mM acetate or 20 mM NH_4Cl (cf. Table II) would correlate best with the relative cell distributions shown at the arrows. Identical nigericin buffers were used to calibrate 2′,7′-bis(carboxyethyl)-5,6-carboxyfluorescein fluorescence measurements of cytoplasmic pH, according to established techniques (55, 75), which further confirmed that 70 mM acetate lowers cytoplasmic pH to ~6.4–6.6 while 20 mM NH_4Cl raises it to ~pH 7.8–8.0 (26).

suggests that lysosomes possess microtubule-based motors that can be influenced by ambient pH. Since lysosomes are normally found around the cell center, and can be seen to move toward the cell center by video microscopy (15, 41), it is likely that they possess retrograde motors of the sort that are generally turning out to be cytoplasmic dyneins (78, 80). On the other hand, since lysosomes also display bidirectional movements in video microscopy (15, 41), and now have been found to move away from the cell center in response to cytoplasmic acidification, they may also possess anterograde motors like kinesin (see reference 78 for an excellent review of these motors). Why lysosomes would have anterograde motors is not established. Perhaps they are needed to move lysosomes to the cell periphery and fuse with incoming endosomes, or perhaps they permit recycling components (e.g., receptors) to move out and reenter the plasma membrane (65). In any case, the net effect of cytoplasmic acidification may be to turn off a retrograde motor associated with lysosomes and/or turn on an associated anterograde motor. Alternatively, acidification could reverse a single bidirectional motor (17). Clearly it will be interesting to learn, in in vitro assays, whether acidity inhibits cytoplasmic dynein relative to kinesin and whether alkalinity does the opposite.

Analogous Organelle Movements in Other Cell Types

The lysosome movements seen here are strikingly similar to the granule movements observed in melanophores and other pigmented cells (9, 34, 35). In the latter, the mechanisms of pigment-granule movement are becoming clarified by the use of detergent-permeabilized cells (37, 42, 61). Such "models" continue to move granules in an ATP-dependent manner and to display bulk redistributions of the granules in response to various experimental manipulations. For example, in melanophore models, pigment dispersal is activated by exogenous cyclic AMP (38, 60), raising the possibility that changes in cyclic AMP are correlated with the pH changes provoked in the present study. In preliminary experiments we have found that applying membrane-permeant dibutyryl-cyclic AMP (1 mM) or forskolin (50 μM) to macrophages

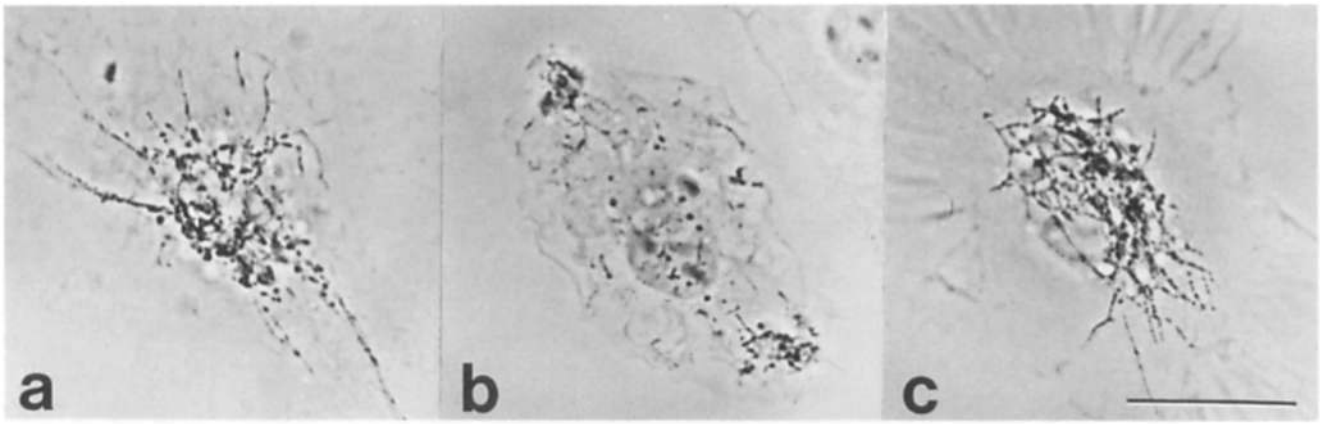

Figure 5. Redistribution of acid phosphate-stained lysosomes in mouse bone marrow macrophages. Here the substrate for acid phosphatase histochemistry was β-glycerophosphate; the substrates cytidine 5′ monophosphate and thiamine pyrophosphate gave identical results. *a* illustrates the predominantly central distribution of lysosomes in an untreated cell. *b* illustrates lysosome breakup and outward movement in a cell treated with 70 mM acetate for 15 min. *c* illustrates return of lysosomes to the cell center and recovery of their tubular forms in a cell permitted to recover for 10 min from previous acetate treatment. Bar, 20 μm.

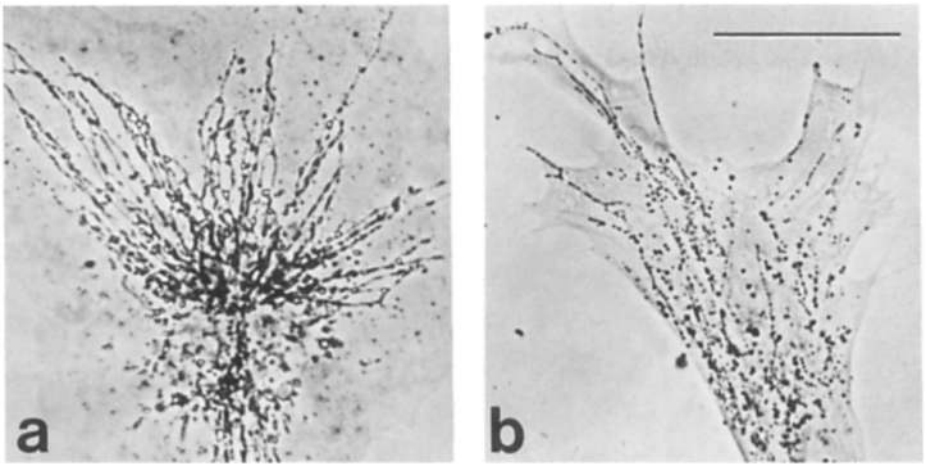

Figure 6. (*a*) Lysosomes appear maximally tubular at ~5 min of recovery from cytoplasmic acidification, particularly in mouse bone marrow macrophages. (*b*) In chick fibroblasts returning lysosomes more often look like beads on a string, presumably due to breakdown of tubules during fixation (cf. references 56, 72). Bar, 20 μm.

also promotes outward movements of lysosomes. However, since the effects of these reagents on cytoplasmic pH have not yet been assessed, it is not clear whether cyclic AMP is promoting a pH drop (30, 54) or vice versa. In any case, it is attractive to speculate that in both pigment cells and cultured cells, cyclic AMP triggers the phosphorylation of protein(s) that inhibit cytoplasmic dynein and/or stimulate kinesin activity.

In a similar vein, images strikingly analogous to the ones shown here were recently published in a study of microtubule-directed outward movement of secretory granules in cultured rat atrial myocytes (28). These movements were induced by treatment with monesin, a Na:H ionophore that is generally thought to provoke cytoplasmic alkalinization (51, 53); however, since monensin also raises intracellular sodium in these cells (27, 28) it may instead acidify them by shutting down their Na:H antiporter (32, 39, 43). In either case, the observed redistribution of secretory granules presumably represents an enhancement of their normal ability to move anterogradely along microtubules (40, 77). It will be interesting to determine whether changes in cytoplasmic pH accompany such movements, in these and other secretory cells.

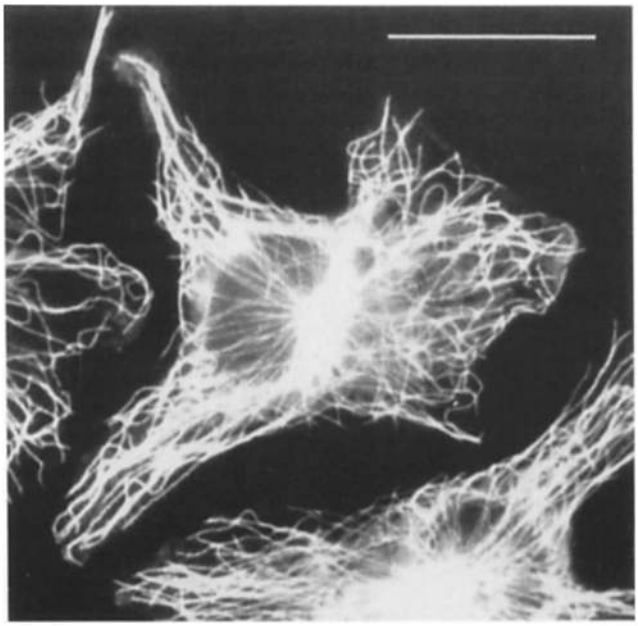

Figure 7. Fluorescence immunocytochemistry of microtubules in mouse bone marrow macrophages. Cells were fixed in −20°C methanol, reacted with 10 μg/ml rabbit polyclonal antitubulin (kindly supplied by M. Kirschner, University of California, San Francisco) and then with rhodamine-conjugated goat anti-rabbit antibody. No changes from this typical abundance and "astral" pattern of radiation were observed during acetate or NH_4Cl treatment. Bar, 20 μm.

Possible Relation of Organelle Redistributions to Membrane Ruffling Activity

The acid-induced redistribution of lysosomes seen here reflects the overall polarity of the cell, in that they accumulate predominantly in regions that were originally ruffling. This is most apparent in J774 macrophages, which tend to ruffle at discrete poles and have microtubules running in bundles from the centrosphere region into these poles (Fig. 2; see also Fig. 7). This polarized microtubule distribution is thought to play a role in targeting the delivery of new membrane to growth areas (8, 31) and in permitting these cells to direct secretion into specific areas were phagocytosis occurs. Thus there may be a link between the peripheral accumulation of organelles and the arrest of membrane ruffling seen here. Possibly, some of the accumulated organelles were destined to discharge in order to support the ruffling, but were prevented from fusing with the plasma membrane by cytoplasmic acidification. This possibility could be evaluated by looking for an enhancement of membrane delivery to the cell surface during acetate washout or during cytoplasmic alkalinization, since both prompt the resumption of unusually active ruffling.

The observed correlation between stimulation of outward organelle movement and inhibition of cell motility is strikingly similar to the behavior of certain neuronal growth cones in culture. Forscher et al. (18) have shown that pharmacological elevation of cyclic AMP in cultured *Aplysia* neurons causes rapid distal migration of organelles into growth cones, again with a concomitant retraction of their ruffles. This yields images of growth cones (Fig. 5 *b* in reference 18) that appear almost identical to the distal processes of acidified macrophages (especially Fig. 2 *b*). Similar movements

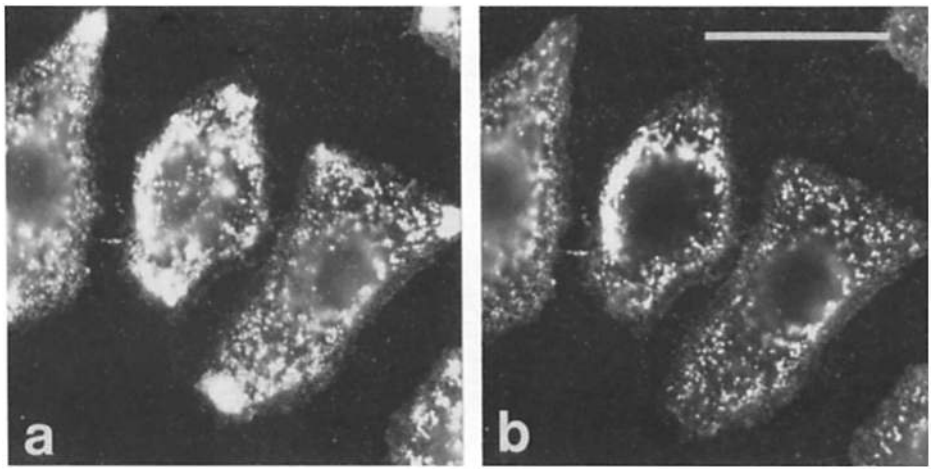

Figure 8. Demonstration that recently formed phagosomes do not accompany lysosomes during acid-induced outward movements. In *a* (originally yellow), lysosomes were labeled with Lucifer Yellow by 30-min incubation and then shifted to the periphery by 5 min of 70 mM acetate. (Bright peripheral clusters of lysosomes can be seen.) During the acetate exposure, rhodamine-tagged latex beads were also supplied. *b* (originally red) illustrates that the resultant phagosomes did not move outwards in acetate (i.e., few rhodamine-labeled organelles are seen in the peripheral areas that appear bright in *a*). Bar, 20 μm.

of organelles into growth cones apparently occur spontaneously during the "consolidation" phase of normal neurite growth (1). Such changes in growth cones develop with the same rapid time course as seen during acidification of macrophages and fibroblasts, and are also reversible. Again, it may turn out that cyclic AMP acidifies growth cones by shutting down their Na:H antiporters (22, 30, 54). In this case, the mechanisms that coordinately alter organelle movement and cell ruffling could turn out to be much the same in all motile cells.

Relating Lysosome Movements to Earlier Observations on Tubular Lysosomes

The astral arrays of HRP-loaded tubular lysosomes seen here during recovery from acidification (Fig. 5), and also seen occasionally in untreated cells (Table II), are very reminiscent of those described earlier in phorbol-treated peritoneal macrophages (49, 72). The latter cells were found to develop radiating arrays of tubular lysosomes as they spread out on the culture dish in response to phorbols (48, 49). The macrophages used here are already as spread out as the phorbol-stimulated ones of these earlier studies, probably due to their long cultivation in CSF-1-containing media (10, 50), and they often display tubular lysosomes at the outset (Tables II and III). The outward movements induced by acidification thus start from this point and proceed to even further lysosome displacement. The deployment of lysosomal tubules has recently been witnessed directly by video microscopy (15) and has been found to be strictly dependent on the presence of microtubules (72), suggesting that it involves an anterograde motor. Since cytoplasmic acidification causes these tubules as well as the more central elements of the lysosomal system to move all the way to the cell periphery, it could be interpreted as excessive stimulation of this same mechanism. Whether this excess also causes the observed breakdown of lysosomal tubules into vesicles remains to be seen. Here, we have not distinguished between the effects of changing cytoplasmic pH and the effects of changing the luminal pH of the lysosomes themselves. Both may have changed in parallel, so the relevant factor controlling lysosome fusion and fission remains unclear.

We could find only two indications in the earlier literature of lysosomal breakup and displacement as extreme as described here. One was Fig. 1 in reference 20, where macrophages were loaded with a relatively high concentration of chlorite-oxidized potato amylose coupled to fluorescein. The other was Fig. 2 *c* in reference 24, where ovarian granulosa cells were exposed to acridine orange to label their lysosomes. Both studies claimed that the peripherally displaced lysosomes moved back to the cell center upon exposure to natural ligands (the ligands were yeast cells in the case of the macrophages and serum plus LDL in the case of granulosa cells). This led the observers to suggest that ligand uptake

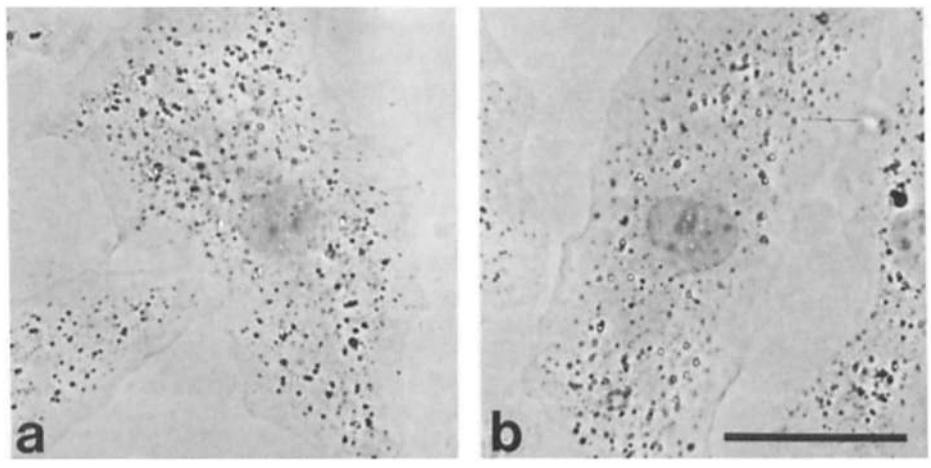

Figure 9. Illustration of the pattern of HRP uptake during acetate treatment rather than before. This restricts the tracer to what are considered to be early endosomes (14, 62). These do not display a tendency to collect peripherally nor to move centrally, unlike more "mature" endosomes and lysosomes. Bar, 20 μm.

somehow induced inward lysosomal movements (20, 24). Based on the present observations, it seems equally likely that either or both methods of labeling lysosomes may have inadvertently acidified the cells in question, thereby inducing lysosome dispersion, and that subsequent exposure to natural ligands simply provided sufficient time for recovery of normal cell pH and normal lysosome centralization. Therefore, in future studies of lysosome shape and distribution, it will clearly be important to determine whether changes in cytoplasmic pH and lumenal pH accompany other experimental manipulations.

Special thanks to Laura Sampson, a Ph.D. candidate in Dr. Eric Brown's laboratory at Washington University, for providing the mouse bone marrow macrophages that were the primary subjects of this study. Thanks also to Robyn Roth and Melisse Reichman for technical assistance, Comfree Colman for photography, Ian Jones for typing, and Drs. A. Roos and P. Schlesinger of this University for advice on methods of altering and measuring cytoplasmic pH.

This work was supported by United States Public Health Service grant GM29647.

Received for publication 19 September 1988 and in revised form 23 November 1988.

References

1. Aletta, J. M., and L. A. Greene. 1988. Growth cone configuration and advance: a time-lapse study using video-enhanced differential interference contrast microscopy. *J. Neurosci.* 8:1425–1435.
2. Araki, N., and K. Ogawa. 1987. Regulation of intracellular lysosomal movements by the cytoskletal system in rat alveolar macrophages. *Acta. Histochem. Cytochem.* 20:654–691.
3. Beaudoin, A. R., G. Grondin, A. Lord, and M. Pelletier. 1985. β-NADPHase and TMPase-positive "snake-like tubules" in the exocrine pancreas. *J. Histochem. Cytochem.* 33:569–575.
4. Bhisey, A. N., and J. J. Freed. 1971. Altered movement of endosomes in colchicine-treated cultured microphages. *Exp. Cell. Res.* 64:430–438.
5. Boron, W. F. 1977. Intracellular pH transients in giant barnacle muscle fibers. *Am. J. Physiol.* 233:C61–C73.
6. Boron, W. F., and P. De Weer. 1976. Intracellular pH transients in squid giant axons caused by CO_2, NH_3, and metabolic inhibitors. *J. Gen. Physiol.* 67:91–110.
7. Brady, S. T. 1985. A novel brain ATPase with properties expected for the fast axonal transport motor. *Nature (Lond.).* 317:73–75.
8. Bretscher, M. S. 1988. Fibroblasts on the move. *J. Cell Biol.* 106:235–237.
9. Byers, H. R., and K. R. Porter. 1977. Transformations in the structure of the cytoplasmic ground substance in erythrophores during pigment aggregation and dispersion. *J. Cell Biol.* 75:541–558.
10. Celada, A., P. W. Gray, E. Rinderknecht, and R. D. Schreiber. 1984. Evidence for a gamma-interferon receptor that regulates macrophage tumoricidal activity. *J. Exp. Med.* 160:55–74.
11. Cohn, Z. A., and B. Benson. 1965. The differentiation of mononuclear phagocytes: morphology, cytochemistry, and biochemistry. *J. Exp. Med.* 121:1953–1970.
12. Cohn, Z. A., and E. Parks. 1967. The regulation of pinocytosis in mouse macrophages. II. Factors inducing vesicle formation. *J. Exp. Med.* 125:213–231.
13. Collot, M., D. Louvard, and S. J. Singer. 1984. Lysosomes are associated with microtubules and not with intermediate filaments in cultured fibroblasts. *Proc. Natl. Acad. Sci. USA.* 81:788–792.
14. Davoust, J., J. Gruenberg, and K. E. Howell. 1987. Two threshold values of low pH block endocytosis at different stages. *EMBO (Eur. Mol. Biol. Organ.) J.* 6:3601–3609.
15. De Brabander, M., R. Nuydens, H. Gurts, and C. R. Hopkins. 1988. Dynamic behavior of the transferrin receptor in living epidermoid carcinoma (A431) cells with nanovid microscopy. *Cell Motil. Cytoskel.* 9:30–47.
16. Essner, E., and H. Haines. 1977. Ultrastructural study of GERL in beige mouse alveolar macrophages. *J. Cell Biol.* 75:381–387.
17. Euteneuer, U., M. P. Koonce, K. K. Pfister, and M. Schliwa. 1988. An ATPase with properties expected for the organelle motor of the giant amoeba, Reticulomyxa. *Nature (Lond.).* 332:176–178.
18. Forscher, P., L. K. Kaczmarek, J. Buchanan, and S. J. Smith. 1987. Cyclic AMP induces changes in distribution and transport of organelles within growth cones of Aplysia bag cell neurons. *J. Neurosci.* 7:3600–3611.
19. Freed, J. J., and M. M. Lebowitz. 1970. The association of a class of saltatory movements with microtubules in cultured cells. *J. Cell Biol.* 45:334–354.
20. Geisow, M. J., G. H. Beaven, P. D. A. Hart, and M. R. Young. 1980. Site of action of a polyanion inhibitor of phagosome-lysosome fusion in cultured macrophages. *Exp. Cell Res.* 126:159–165.
21. Griffiths, G., B. Hoflack, K. Simons, I. Mellman, and S. Kornfeld. 1988. The mannose 6-phosphate receptor and the biogenesis of lysosomes. *Cell.* 52:329–341.
22. Grinstein, S., and A. Rothstein. 1986. Mechanisms of regulation of the Na^+/H^+ exchanger. *J. Membr. Biol.* 90:1–12.
23. Hart, P. D. A., M. R. Young, M. M. Jordan, W. J. Perkins, and M. J. Geisow. 1983. Chemical inhibitors of phagosome-lysosome fusion in cultured macrophages also inhibit saltatory lysosomal movements. *J. Exp. Med.* 158:477–492.
24. Herman, B., and D. F. Albertini. 1984. Time-lapse video image intensification analyses of cytoplasmic organelle movements during endosome translocation. *J. Cell Biol.* 98:565–576.
25. Heuser, J. E., and T. S. Reese. 1973. Evidence for recycling of synaptic vesicle membrane during transmitter release at the frog neuromuscular junction. *J. Cell Biol.* 57:315–344.
26. Heuser, J. 1989. Effects of cytoplasmic acidification on clathrin lattice morphology. *J. Cell Biol.* 108:401–411.
27. Hume, J. R., and A. Uehara. 1986. Properties of "creep currents" in single frog atrial cells. *J. Gen. Physiol.* 87:833–884.
28. Ida, H., W. W. Barron, and E. Page. 1988. Monensin turns on microtubule-associated translocation of secretory granules in cultured rat atrial myocytes. *Circ. Res.* 62:1159–1170.
29. Kachar, B., J. P. Albanesi, H. Fujisaki, and E. D. Korn. 1987. Extensive purification from Acanthamoeba of a microtubule-dependent translocator with ATPase activity. *J. Biol. Chem.* 262:16180–16185.
30. Kahn, A. M., G. M. Dolson, M. K. Hise, S. C. Bennett, and E. J. Weinman. 1985. Parathyroid hormone and dibutyryl cAMP inhibit Na^+/H^+ exchange in renal brush border vesicles. *Am. J. Physiol.* 248:F212–F218.
31. Kupfer, A., P. J. Kronebusch, J. K. Rose, and S. J. Singer. 1987. A critical role for the polarization of membrane recycling in cell motility. *Cell Motil. Cytoskeleton.* 8:182–189.
32. L'Allemain, G., S. Paris, and J. Pouysségur. 1984. Growth factor action and intracellular pH regulation in fibroblasts. *J. Biol. Chem.* 259:5809–5815.
33. Lewis, W. H. 1931. Pinocytosis. *Bull. Johns Hopkins Hosp.* 49:17–27.
34. Luby, K. H., and K. R. Porter. 1980. The control of pigment migration in isolated erythrophores of Holocentrus. I. Energy requirements. *Cell.* 21:13–23.
35. Luby-Phelps, K., and K. R. Porter. 1982. The control of pigment migration in isolated erythrophores of Holocentrus. II. The role of calcium. *Cell.* 29:441–450.
36. Lye, R. J., M. E. Porter, J. M. Scholey, and J. R. McIntosh. 1987. Identification of a microtubule-based cytoplasmic motor in the Nematode C. Elegans. *Cell.* 51:309–318.
37. Lynch, T. J., J. D. Taylor, and T. T. Tchen. 1986. Regulation of pigment organelle translocation. I. Phosphorylation of the organelle associated protein p57. *J. Biol. Chem.* 261:4204–4211.
38. Lynch, T. J., B.-Y. Wu, S. D. Taylor, and T. T. Tchen. 1986. Regulation of pigment organelle translocation. II. Participation of a c-AMP dependent protein kinase. *J. Biol. Chem.* 261:4212–4216.
39. Mahnensmith, R. L., and P. S. Aronson. 1986. The plasma membrane sodium-hydrogen exchanger and its role in physiological and pathophysiological processes. *Circ. Res.* 56:773–788.
40. Mains, R. E., and V. May. 1988. The role of a low pH intracellular compartment in the processing, storage and secretion of ACTH and endorphin. *J. Biol. Chem.* 263:7887–7894.
41. Matteoni, R., and T. E. Kreis. 1987. Translocation and clustering of endosomes and lysosomes depends upon microtubules. *J. Cell Biol.* 105: 1253–1265.
42. McNivin, M. A., and J. B. Ward. 1988. Calcium regulation of pigment transport in vitro. *J. Cell Biol.* 106:111–125.
43. Moolenaar, W. H., R. Y. Tsien, P. T. van der Saag, and S. W. de Laat. 1983. Na^+/H^+ exchange and cytoplasmic pH in the action of growth factors in human fibroblasts. *Nature (Lond.).* 304:645–648.
44. Mueller, S. C., and A. L. Hubbard. 1986. Receptor-mediated endocytosis of asialoglycoproteins by rat hepatocytes: receptor-positive and receptor-negative endosomes. *J. Cell Biol.* 102:932–942.
45. Oliver, C. 1980. Cytochemical localization of acid phosphatase and trimetaphosphatase activities in exocrine acinar cells. *J. Histochem. Cytochem.* 28:78–81.
46. Oliver, C. 1983. Characterization of basal lysosomes in exocrine acinar cells. *J. Histochem. Cytochem.* 31:1209–1216.
47. Pastan, I., and M. C. Willingham. 1981. Journey to the center of the cell: role of the receptosome. *Science (Wash. DC).* 214:504–506.
48. Phaire-Washington, L., E. Wang, and S. Silverstein. 1980. Phorbol myristate acetate stimulates pinocytosis and membrane spreading in mouse peritoneal macrophages. *J. Cell Biol.* 86:634–640.
49. Phaire-Washington, L., S. C. Silverstein, and E. Wang. 1980. Phorbol myristate acetate stimulates microtubule and 10 nm filament extension and lysosome redistribution in mouse macrophages. *J. Cell Biol.* 86:641–655.

50. Portnoy, D. A., P. S. Jacks, and D. J. Hinrichs. 1988. Role of hemolysin for the intracellular growth of Listeria monocytogenes. *J. Exp. Med.* 167:1459–1471.
51. Pressman, B. C., E. J. Harris, W. S. Jagger, and J. H. Johnson. 1967. Antibiotic-mediated transport of alkali ions across lipid barriers. *Proc. Natl. Acad. Sci. USA.* 58:1949–1956.
52. Ralph, P., and I. Nakoinz. 1975. Phagocytosis and cytolysis by a macrophage tumor and its cloned cell line. *Nature (Lond.).* 257:393–394.
53. Reed, P. W. 1979. Ionophores. *Methods. Enzymol.* 55:435–453.
54. Reuss, L., and K.-U. Petersen. 1985. Cyclic AMP inhibits Na^+/H^+ exchange at the apical membrane of Necturus gallbladder epithelium. *J. Gen. Physiol.* 85:409–429.
55. Rink, T. J., R. Y. Tsien, and T. Pozzan. 1982. Cytoplasmic pH and free Mg^{++} in lymphocytes. *J. Cell Biol.* 95:189–196.
56. Robinson, J. M., T. Okada, J. J. Castellot, and M. J. Karnovsky. 1986. Unusual lysosomes in aortic smooth muscle cells: presence in living and rapidly frozen cells. *J. Cell Biol.* 102:1615–1622.
57. Rogers, J., T. R. Hesketh, G. A. Smith, M. A. Beaven, J. C. Metcalfe, P. Johnson, and P. B. Garland. 1983. Intracellular pH and free calcium changes in single cells using guin 1 and quin 2 probes and fluorescence microscopy. *FEBS (Fed. Eur. Biochem. Soc.) Lett.* 161:21–27.
58. Rogers, J., T. R. Hesketh, G. A. Smith, and J. C. Metcalfe. 1983. Intracellular pH of stimulated thymocytes measured with a new fluorescent indicator. *J. Biol. Chem.* 258:5994–5997.
59. Roos, A., and W. F. Boron. 1981. Intracellular pH. *Physiol. Rev.* 61:296–434.
60. Rozdzial, M. M., and L. T. Haimo. 1986. Bidirectional pigment granule movements of melanophores are regulated by protein phosphorylation and dephosphorylation. *Cell.* 47:1061–1070.
61. Rozdzial, M. M., and L. T. Haimo. 1986. Reactivated melanophore motility: differential regulation and nucleotide requirements of bidirectional pigment granule transport. *J. Cell Biol.* 103:2755–2764.
62. Samuelson, A. C., R. J. Stockert, A. B. Novikoff, P. M. Novikoff, J. C. Saez, D. C. Spray, and A. W. Wolkoff. 1988. Influence of cytosolic pH on receptor-mediated endocytosis of asialoorosomucoid. *Am. J. Physiol.* 254:C829–C838.
63. Sandvig, K., S. Olsnes, O. W. Peterson, and B. van Deurs. 1987. Acidification of the cytosol inhibits endocytosis from coated pits. *J. Cell Biol.* 106:679–689.
64. Schmid, S. L., R. Fuchs, P. Male, and I. Mellman. 1988. Two distinct subpopulations of endosomes involved in membrane recycling and transport to lysosomes. *Cell.* 52:73–83.
65. Schneider, Y.-J., P. Tulkens, C. De Duve, and A. Trout. 1979. Fate of plasma membrane during endocytosis: evidence for recycling of plasma membrane constituents. *J. Cell Biol.* 82:466–474.
66. Scholey, J. M., M. E. Porter, P. M. Grissom, and J. R. McIntosh. 1985. Identification of kinesin in sea urchin eggs, and evidence for its localization in the mitotic spindle. *Nature (Lond.).* 318:483–486.
67. Sorokin, S. P. 1976. A labyrinthian procursor of primary lysosomes in alveolar macrophages. *J. Cell Biol.* 70:381*a*.
68. Steinman, R. M., and Z. A. Cohn. 1972. The interaction of soluble horseradish peroxidase with mouse peritoneal macrophages in vitro. *J. Cell Biol.* 55:186–204.
69. Steinman, R. M., J. M. Silver, and Z. A. Cohn. 1974. Pinocytosis in fibroblasts. Quantitative studies in vitro. *J. Cell Biol.* 63:949–969.
70. Steinman, R. M., S. E. Brodie., and Z. A. Cohn. 1976. Membrane flow during pinocytosis: a stereologic analysis. *J. Cell Biol.* 68:665–687.
71. Steinman, R. M., I. S. Mellman, W. A. Muller, and Z. A. Cohn. 1983. Endocytosis and the recycling of plasma membrane. *J. Cell Biol.* 96:1–27.
72. Swanson, J., A. Bushnell, and S. C. Silverstein. 1987. Tubular lysosome morphology and distribution within macrophages depends on integrity of cytoplasmic microtubules. *Proc. Natl. Acad. Sci. USA.* 84:1921–1925.
73. Terasaki, M., J. Song, J. R. Wong, M. J. Weiss, and L. B. Chen. 1984. Localization of endoplasmic reticulum in living and glutaraldehyde fixed cells with fluorescent dyes. *Cell.* 38:101–108.
74. Terasaki, M., L. B. Chen, and K. Fujiwara. 1986. Microtubules and the endoplasmic reticulum are highly interdependent structures. *J. Cell Biol.* 103:1557–1568.
75. Thomas, J. A., R. N. Buchsbaum, A. Zimniak, and E. Racker. 1979. Intracellular pH measurements in Ehrlich ascites tumor cells utilizing spectroscopic probes generated *in situ*. *Biochemistry.* 18:2210–2218.
76. Thomas, J. A., P. C. Kolbeck, and T. A. Langworthy. 1982. Spectrophotometric determination of cytoplasmic and mitochondrial pH transitions using trapped pH indicators. *In* Intracellular pH: Its Measurement, Regulation and Utilization in Cellular Functions. R. Nuccitelli and D. W. Deamer, editors. Alan R. Liss, Inc. NY. 105–123.
77. Tooze, J., and B. Burk. 1987. Accumulation of adrenocorticotropin secretory granules in the midbody of telophase AtT20 cells: evidence that secretory granules move anterogradely along microtubules. *J. Cell Biol.* 104:1047–1057.
78. Vale, R. D. 1987. Intracellular transport using microtubule-based motors. *Annu. Rev. Cell Biol.* 3:347–378.
79. Vale, R. D., T. S. Reese, and M. P. Sheetz. 1985. Identification of a novel force-generating protein, kinesin, involved in microtubule-based motility. *Cell.* 42:39–50.
80. Vale, R. D., B. J., Schnapp, T. Mitchison, E. Steuer, T. S. Reese, and M. P. Sheetz. 1985. Different axoplasmic proteins generate movement in opposite directions along microtubules in vitro. *Cell.* 43:623–632.
81. Wolkoff, A. W., R. D. Klausner, G. Ashwell, and J. Harford. 1984. Intracellular segregation of asialoglycoproteins and their receptor: a prelysosomal event subsequent to dissociation of the ligand-receptor complex. *J. Cell Biol.* 98:375–381.